Perovskites Hot Paper

Deutsche Ausgabe: DOI: 10.1002/ange.201504784
Internationale Ausgabe: DOI: 10.1002/anie.201504784

Rattling in the Quadruple Perovskite $CuCu_3V_4O_{12}$

Yasuhide Akizuki, Ikuya Yamada, Koji Fujita,* Kazuya Taga, Takateru Kawakami, Masaichiro Mizumaki, and Katsuhisa Tanaka*

Abstract: *Of particular interest is a peculiar motion of guest atoms or ions confined to nanospace in cage compounds, called rattling. While rattling provides unexplored physical properties through the guest–host interactions, it has only been observed in a very limited class of materials. Herein, we introduce an A-site-ordered quadruple perovskite, $CuCu_3V_4O_{12}$, as a new family of cage compounds. This novel $AA'_3B_4O_{12}$-type perovskite has been obtained by a high-pressure synthesis technique and structurally characterized to have cubic $Im\bar{3}$ symmetry with an ionic model of $Cu^{2+}Cu^{2+}{}_3V^{4+}{}_4O_{12}$. The thermal displacement parameter of the A-site Cu^{2+} ion is as large as $U_{iso} \approx 0.045$ Å^2 at 300 K, indicating its large-amplitude thermal oscillations in the oversized icosahedral cages. Remarkably, the presence of localized phonon modes associated with rattling of the A-site Cu^{2+} ion manifests itself in the low-temperature specific heat data. This work sheds new light on the structure–property relations in perovskites.*

Material classes, such as $VAl_{10+\delta}$, filled skutterudites, clathrates, and β-pyrochlore oxides have attracted much interest. The structures of these compounds are commonly characterized by a three-dimensional network of polyhedral cages that are capable of endohedrally accommodating guest ions.[1] The guest, if it is undersized relative to the cage, can vibrate anharmonically with low frequency and large amplitude, independent of other guests.[1a,2–16] Such local anharmonic vibrations, often referred to as rattling, are believed to bring about several intriguing phenomena, such as strong scattering of long-wavelength acoustic phonons,[17] superconductivity,[12,18] and sizeable electron-mass enhancement.[12,18b,c,19]

The aristotype of the ABO_3 perovskites (space group $Pm\bar{3}m$) has twelve-fold cuboctahedral *A*-site cavities. If undersized cations were introduced into the *A*-site as guest ions without distorting the cavities, they would behave as rattlers; however, such a situation has not been realized in real perovskites. This is because, when the size of *A*-site cations becomes so small for the cuboctahedral cavity, various types of tilting or rotating of BO_6 octahedra induce a distortion of AO_{12} polyhedra, which hampers the production of the large space required for the cations to exhibit local vibrations. On the other hand, it may be feasible to avoid such a situation in *A*-site-ordered perovskite oxides with formula unit $AA'_3B_4O_{12}$, the focus of this study, instead of simple perovskite oxides. Of great interest is the structural similarity of the quadruple perovskites to the filled skutterudites LnT_4X_{12} (Ln = lanthanide, T = transition metal, X = pnictogen) where the Ln atom rattles within the oversized X_{12} icosahedral cage; both compounds crystallize in the cubic space group $Im\bar{3}$,[1b,20] with *A* and Ln, *B* and T, and O and X atoms being located at 2*a* (0, 0, 0), 8*c* (1/4, 1/4, 1/4), and 24*g* (0, *y*, *z*) sites, respectively. As a result of materials exploration using high-pressure synthesis, it is now possible to obtain numerous members in the $AA'_3B_4O_{12}$ family, especially compounds with Jahn–Teller active cations (Cu^{2+} or Mn^{3+}) occupying the *A*′-site. In these perovskites containing transition-metal cations on both *A*′- and *B*-sites, the BO_6 octahedral network is heavily tilted because of the square-planar $A'O_4$ coordination preferred by the *A*′-site cations (see Figure 1c). Because of this structural feature, the icosahedrally twelve-coordinated *A*-site can accommodate a wide range of cations of different sizes, while retaining the cubic $Im\bar{3}$ symmetry. For example, the $Im\bar{3}$ perovskite structure can be obtained for Ln ions of different sizes,[21] and tolerates even a full vacancy on the *A*-site (e.g., $\square Cu_3Ti_2Ta_2O_{12}$[20b]). This motivated us to examine the possible rattling of *A*-site cations in $AA'_3B_4O_{12}$ perovskites.

Very recently, it has been reported that small transition-metal cations can be incorporated even into the icosahedrally coordinated *A*-site in $AA'_3B_4O_{12}$-type perovskites.[22] We synthesized a cubic $Im\bar{3}$ $MnCu_3V_4O_{12}$ under 12 GPa at elevated temperatures.[22b] Mn^{2+} has the smallest ionic radius of the cations found on the *A*-site, and its thermal displacement parameter at 300 K is fairly large ($U_{iso} \approx 0.02$ Å^2) compared to those of the other cations, that is, Cu^{2+} and V^{4+} ($U_{iso} < 0.005$ Å^2), showing the thermal oscillations of Mn^{2+} ions in the icosahedral cages. In the temperature-dependent specific heat (C_p) data, however, specific vibrational excitations associated with the local motions of Mn^{2+} ions were not detected.

[*] Dr. Y. Akizuki, Dr. K. Fujita, K. Taga, Prof. K. Tanaka
Graduate School of Engineering
Kyoto University
Kyoto 615-8510 (Japan)
E-mail: fujita@dipole7.kuic.kyoto-u.ac.jp
Dr. I. Yamada
Nanoscience and Nanotechnology Research Center
Osaka Prefecture University
1-2 Gakuen-cho, Nakaku, Sakai, Osaka 599-8531 (Japan)
and
JST-PRESTO
4-1-8 Honcho Kawaguchi, Saitama 332-0012 (Japan)
E-mail: i-yamada@21c.osakafu-u.ac.jp
Dr. T. Kawakami
College of Humanities and Sciences, Nihon University
Tokyo 156-8550 (Japan)
Dr. M. Mizumaki
Japan Synchrotron Radiation Research Institute
SPring-8, Hyogo 679-5148 (Japan)

Supporting information for this article is available on the WWW under http://dx.doi.org/10.1002/anie.201504784.

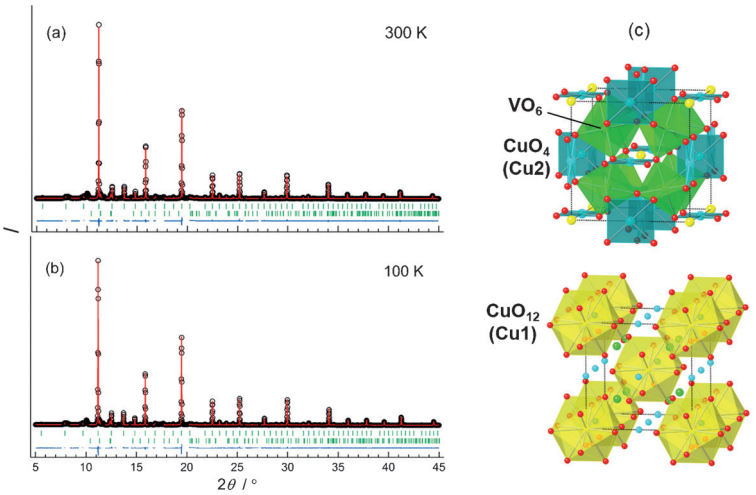

Figure 1. Rietveld refinement of SXRD patterns ($\lambda = 0.50015$ Å) of $CuCu_3V_4O_{12}$ at a) 300 K and b) 100 K. The observed (open circle) and calculated (red line) patterns and the difference (bottom blue line) between them are shown. The reflection positions of $CuCu_3V_4O_{12}$ are marked with the upper green ticks. A small amount of impurity phase CuO (ca. 7.0 wt%: reflection positions are marked with lower green ticks) is included in the refinement, and unknown phases are excluded from the refinement. c) The refined crystal structure of $CuCu_3V_4O_{12}$ highlighting the CuO_4 planes and VO_6 octahedral units (upper) and the CuO_{12} icosahedral units (lower). Spheres: Cu1 (*A*-site) yellow, Cu2 (*A′*-site) blue, O red, V (*B*-site) green

Herein, we report on the high-pressure synthesis of a novel isostructural perovskite with a smaller *A*-site cation, $CuCu_3V_4O_{12}$. Our structural characterizations show that this quadruple perovskite has a valence distribution of $Cu^{2+}Cu^{2+}{}_3V^{4+}{}_4O_{12}$, representing the first example of a perovskite oxide in which small Cu^{2+} ions occupy the twelve-coordinate *A*-site. Remarkably, the rattling of *A*-site Cu^{2+} ions shows up in the low-temperature C_p data as Einstein-like vibrational modes.

Samples were synthesized by the solid-state reaction at 15 GPa and 1523 K using a Kawai-type high-pressure apparatus. The synchrotron powder X-ray diffraction (SXRD) pattern at 300 K (Figure 1a) reveals the superstructure peaks associated with the *A*-site cationic ordering that leads to an enlarged $2a_p \times 2a_p \times 2a_p$ unit cell (relative to its archetype with a lattice parameter a_p), indicating the formation of a cubic $AA'_3B_4O_{12}$-type perovskite structure with lattice constant of $a \approx 7.28$ Å. There is no signature of any structural transition down to 100 K (Figure 1b). Although an ilmenite-type $CuVO_3$ (space group $R\bar{3}$) was synthesized at a pressure of approximately 6 GPa,[23] our investigation demonstrates that applying higher pressures up to 15 GPa leads to the formation of the perovskite phase. The calculated density is larger for the perovskite phase (5.668 g cm^{-3}) than for the ilmenite phase (5.411 g cm^{-3}), indicating that the perovskite is a higher-density phase stabilized under the higher pressure.

We initially refined the SXRD pattern at 300 K using the $Im\bar{3}$ structure model in which *A*-site Cu (Cu1), *A′*-site Cu (Cu2), *B*-site V, and O atoms were placed at 2*a*, 6*b*, 8*c*, and 24*g* positions, respectively. Refinement converged well with a weight reliability factor of $R_{wp} = 5.872\,\%$, but the atomic displacement parameter of $U_{iso} = 0.0446(9)$ Å^2 for Cu1 was unusually large compared to those for Cu2, V, and O ($U_{iso} = 0.0027$–0.0052 Å^2). Such a large U_{iso} value is caused by either static disorder or thermal vibrations. For the static disorder, we first examined the possibility of Cu1 deficiency, but there was no deviation from the site occupancy $g(\mathrm{Cu1}) = 1$ in the trial refinements. Then, we checked split-site models with Cu1 displacements, but none of their models improved the *R* factors (Supporting Information, Table S1). This precludes a possibility of Cu1 displacive disorder, and thus, it is reasonable to consider that the thermal vibration of Cu1 leads to the large U_{iso} value. The dynamic Cu1 oscillation also shows up as an unusual behavior in the C_p data as described below. Using the ideal-position model, we were careful to refine the data between 100 and 450 K in a consistent manner. The final refinement results at 300 and 100 K are listed in Table 1 as representative examples. Figure 1c illustrates the refined crystal structure of $CuCu_3V_4O_{12}$, in which Cu atoms occupy both the square-coordinated *A′*-site and icosahedrally twelve-coordinated *A*-site.

The bond valence sums (BVSs)[24] calculated from the metal–oxygen bond lengths in $CuCu_3V_4O_{12}$ are 1.09, 2.22, and 4.18 for Cu1, Cu2, and V, respectively. The BVS values for Cu2 and V are very close to those for Cu (2.19) and V (4.11) in an isostructural compound $Ca^{2+}Cu^{2+}{}_3V^{4+}{}_4O_{12}$,[25] implying that the *A′*-site in $CuCu_3V_4O_{12}$ is Cu^{2+} and the *B*-site cation is V^{4+}. On the other hand, the BVS value for Cu1 is much lower than the valence state of the *A*-site cation expected from the charge balance required for $Cu^{2+}Cu^{2+}{}_3V^{4+}{}_4O^{2-}{}_{12}$. To elucidate the Cu valence, we performed X-ray absorption spectroscopy (XAS) at room temperature. Figure 2a displays the Cu *K*-edge XAS spectrum for $CuCu_3V_4O_{12}$, along with those of

Table 1: Refined structure parameters, selected bond lengths, and bond angles at 300 and 100 K for $CuCu_3V_4O_{12}$.[a]

Parameter	300 K	100 K
a [Å]	7.24828(12)	7.23539(12)
y(O)	0.1812(3)	0.1809(4)
z(O)	0.3023(4)	0.3021(4)
U_{iso} (Cu1) [$\times 10^{-2}$ Å^2]	4.46(9)	2.43(8)
U_{iso} (Cu2) [$\times 10^{-2}$ Å^2]	0.33(2)	0.11(2)
U_{iso} (V) [$\times 10^{-2}$ Å^2]	0.52(2)	0.25(2)
U_{iso} (O) [$\times 10^{-2}$ Å^2]	0.27(5)	0.02(5)
Cu1-O [Å]	2.555(3)	2.548(3)
Cu2-O [Å]	1.943(2)	1.940(2)
Cu2-O [Å]	2.719(3)	2.717(3)
V-O [Å]	1.9174(7)	1.9141(7)
∡V-O-V [°]	141.86(18)	141.81(18)

[a] Space group: $Im\bar{3}$ (No. 204). Atomic sites: Cu1 2*a* (0, 0, 0), Cu2 6*b* (0, $^1/_2$, $^1/_2$), V 8*c* ($^1/_4$, $^1/_4$, $^1/_4$), and O 24*g* (0, *y*, *z*). The occupancy factor *g* was fixed to unity for all the sites. $R_{wp} = 5.872\,\%$, $R_B = 2.283\,\%$, and $S = 1.936$ for 300 K, and $R_{wp} = 6.475\,\%$, $R_B = 2.298\,\%$, and $S = 2.100$ for 100 K.

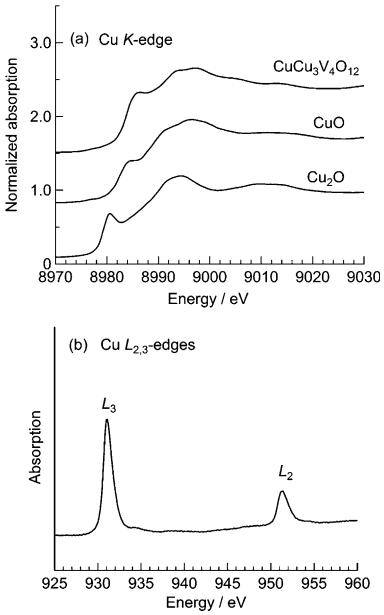

Figure 2. a) Room-temperature XAS spectra at the Cu *K*-edge for $CuCu_3V_4O_{12}$ and standards (CuO and Cu_2O); spectra vertically offset for clarity. b) Room-temperature XAS spectrum at the Cu $L_{2,3}$-edges for $CuCu_3V_4O_{12}$.

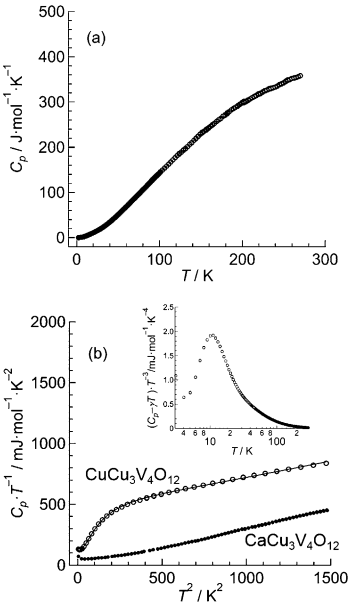

Figure 3. a) Temperature dependence of C_p of $CuCu_3V_4O_{12}$. b) C_p/T versus T^2 plots for $CuCu_3V_4O_{12}$ and $CaCu_3V_4O_{12}$ below 40 K. The solid curve was drawn by fitting Equation (1) to the experimental data of $CuCu_3V_4O_{12}$. Inset: $(C_p-\gamma T)/T^3$ versus T on a logarithmic scale for $CuCu_3V_4O_{12}$.

CuO and Cu_2O standards. The spectral shape of $CuCu_3V_4O_{12}$ resembles that of CuO, rather than that of Cu_2O. It is well established that the edge position shifts toward the higher energy with increasing the Cu valence state;[26] for the XAS spectra of Cu_2O and CuO (Figure 2a), the edge position evaluated from the maximum point of the first derivative is about 8980 and 8984 eV, respectively. The edge position for $CuCu_3V_4O_{12}$ (ca. 8984 eV) is very close to that for CuO, indicating a Cu^{2+} valence state in $CuCu_3V_4O_{12}$. Further evidence for the Cu valence is provided by the Cu $L_{2,3}$-edge XAS spectrum (Figure 2b), which shows a single, symmetrical peak on each edge, in good agreement with the spectral features of isostructural Cu^{2+}-containing oxides, such as $CaCu_3Ti_4O_{12}$[27] and $CaCu_3V_4O_{12}$.[28] For Cu^{3+}-containing oxides, such as $LaCuO_3$ and $LnCu_3Fe_4O_{12}$ (Ln = La–Tb), it has been reported that the main peak at the L_3-edge (ca. 931 eV) is accompanied by a shoulder or an additional peak on its high-energy side,[21b,29] although such a spectral feature is not observed for $CuCu_3V_4O_{12}$. Thus, the XAS results allow us to conclude that both the *A*-site Cu (Cu1) and *A*′-site Cu (Cu2) adopt a valence state of +2, thus excluding the presence of Cu^+ and Cu^{3+} ions. From the XAS analysis and BVS calculations, we assume an ionic model of $Cu^{2+}Cu^{2+}{}_3V^{4+}{}_4O_{12}$; the BVS value of 1.09 for *A*-site Cu (Cu1) reflects the underbonded Cu^{2+}, rather than Cu^+. It is surprising that Cu^{2+} with a $3d^9$ electronic configuration resides in the highly symmetrical twelve-coordinated environment.

Temperature dependence of the specific heat C_p of $CuCu_3V_4O_{12}$ (Figure 3a) shows no clear anomalies ascribable to structural and magnetic phase transitions down to 2 K. Figure 3b depicts the C_p/T versus T^2 plot between 2 and 40 K. The data of an isostructural $CaCu_3V_4O_{12}$ are also depicted for comparison. There is a significant difference in the low-temperature behavior between $CuCu_3V_4O_{12}$ and $CaCu_3V_4O_{12}$. The data for $CaCu_3V_4O_{12}$ approximately follow $C_p/T = \gamma + \beta T^2$ as a result of the contributions of conduction electrons and a Debye-type acoustic phonon; the Sommerfeld coefficient of $\gamma = 18.1(1.2)\ \mathrm{mJ\,mol^{-1}\,K^{-2}}$ is almost the same as that reported previously ($\gamma \approx 30\ \mathrm{mJ\,mol^{-1}\,K^{-2}}$),[25] and the Debye temperature is evaluated to be $\Theta_D = 549(2)$ K from β using the relation $\Theta_D = (12\pi^4 NR/5\beta)^{1/3}$, where N is the number of atoms per unit cell and R is the universal gas constant. In contrast, $CuCu_3V_4O_{12}$ exhibits a concave-down C_p/T–T^2 curve, which immediately evokes a low-frequency enhancement of vibrational density of states.

Although rattling is a local and essentially anharmonic vibration, it can be often approximated by an Einstein mode within a harmonic approximation. If we assume a simple Debye solid with rattlers behaving like Einstein oscillators with a mixing ratio $r(\leq 1)$ and consider the presence of conduction electrons, the specific heat at low temperatures can be described by Equation (1):[2,6]

$$C_p = (12\pi^4/5)(20-r)R(T/\Theta_D)^3 + 3rR(\Theta_E/T)^2\exp(\Theta_E/T)/(\exp(\Theta_E/T)-1)^2 + \gamma T \quad (1)$$

where Θ_E is the Einstein temperature and γ the Sommerfeld coefficient. The electronic contribution γT is considered in the present analysis because $CuCu_3V_4O_{12}$ exhibits the metallic conduction (Supporting Information, Figure S2) and its magnetic susceptibility data involve a Pauli paramagnetism contribution (Figure S3). From the fit of Equation (1) to the C_p/T–T^2 data (Figure 3b, solid curve), we determined $r = 0.427(3)$, $\Theta_E = 55.1(3)$ K, $\Theta_D = 486.0$ (1.1) K, and $\gamma = 126.9$ (1.9) $\mathrm{mJ\,mol^{-1}\,K^{-2}}$. The Debye temperature is very close to

those derived from the C_p data for isostructural perovskites, such as $CaCu_3V_4O_{12}$ and $CaCu_3Ru_4O_{12}$ ($\Theta_D = 451$–549 K),[30] and the Einstein temperature is on the same order of magnitude as those for weakly bound guest atoms (i.e., rattlers) in cage compounds including $VAl_{10+\delta}$ ($\Theta_E \approx 22$ K),[1a,16] filled skutterudites $LnOs_4Sb_{12}$ (Ln = La, Ce, Pr, and Nd; $\Theta_E = 69$–45 K),[14,15,19b] clathrates $M_8Ga_{16}Ge_{30}$ (M = Ba and Sr; $\Theta_E = 60$–53 K),[5] and β-pyrochlore oxides ROs_2O_6 (R = Cs, Rb, and K; $\Theta_E = 70$–31 K).[11,12] Considering the atomic fraction of A-site Cu^{2+} in $CuCu_3V_4O_{12}$, the value of r obtained from fitting seems to be physically meaningful; the unit cell contains 20 atoms, 1 atom of which is Cu1. Thus, the unusual behavior of the C_p data, together with the large value of U_{iso} for Cu1, leads us to conclude that the local modes in $CuCu_3V_4O_{12}$ are best described as "rattling" of A-site Cu^{2+} ions. The dominance of local modes is also corroborated by a bell-shaped feature around 10 K in the $(C_p - \gamma T)/T^3$ versus T on a logarithmic scale (Figure 3b, inset). Such a feature is not described by the Debye-type phonon, but it is pronounced in the presence of rattling.[8,9,11,12,14] From the C_p data analysis, we also find that the Sommerfeld coefficient for $CuCu_3V_4O_{12}$ ($\gamma \approx 126$ mJ mol^{-1} K^{-2}) is relatively large compared to those for isostructural metallic perovskites such as $CaCu_3V_4O_{12}$ ($\gamma =$ 18–30 mJ mol^{-1} K^{-2}) and $CaCu_3Ru_4O_{12}$ ($\gamma = 85$–92 mJ mol^{-1} K^{-2}).[30,31]

In light of the evidence of rattling, we confirmed the temperature dependence of the atomic displacement parameter U_{iso} for each atom in $CuCu_3V_4O_{12}$ (Figure 4). One can see

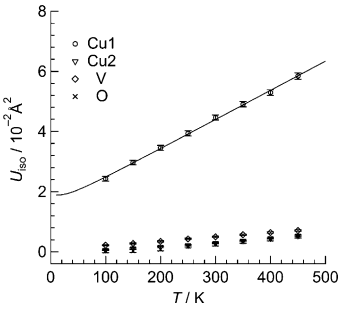

Figure 4. Temperature dependence of U_{iso} of *A*-site Cu (Cu1), *A*′-site Cu (Cu2), *B*-site V, and O atoms, as determined from Rietveld refinement of SXRD data of $CuCu_3V_4O_{12}$. The solid curve represents the fitting of Equation (2) to the Cu1 data.

much larger values of U_{iso} for Cu1 compared to those for Cu2, V, and O over the whole temperature range. This observation is a common feature for rattlers in cage compounds.[1d,5,7,15,16,17d,e,f,19b] We analyzed the U_{iso} data for Cu1 using an Einstein model [Eq. (2)]:

$$U_{iso} = u_0^2 + (\hbar^2/2 m_{Cu} k_B \Theta_E) \coth(\Theta_E/2T) \quad (2)$$

where u_0 is the temperature-independent parameter, $\hbar$ the reduced Plank's constant, k_B the Boltzmann constant, and m_{Cu} the mass of Cu atom. Fitting Equation (2) to the experimental data (Figure 4, solid curve) yields $u_0 = 0.120(1)$ Å and $\Theta_E =$ 88.5(7) K. The Einstein temperature is comparable to that derived from the C_p data analysis ($\Theta_E \approx 55$ K). The large value of u_0 implies that the dynamic Cu1 vibration occurs even at low temperatures, as the contribution of the static Cu1 disorder is insignificant.

To highlight the effect of the size of the A-site cation on rattling in $CuCu_3V_4O_{12}$, we estimated the cation size mismatch at the A-sites in an isostructural series of $ACu_3V_4O_{12}$ perovskites (A = Cu, Mn, and Ca), among which $CuCu_3V_4O_{12}$ alone displays a signature of rattling in the C_p data. A simple measure of the cage size is $d_{cage} = d - r(O^{2-})$,[14,15] where d is the A–O bond length determined from the structure refinement (see Table 1 for A = Cu, Table 1 in Ref. [22b] for A = Mn, and Table S2 in Supporting Information for A = Ca) and $r(O_2)$ is the ionic radius of O^{2-} (1.4 Å). The difference between the d_{cage} value and the ionic radius of A-site cation (Shannon ionic radii for six coordination[32]) is $\Delta = 0.15$ Å for $CaCu_3V_4O_{12}$, $\Delta = 0.34$ Å for $MnCu_3V_4O_{12}$, and $\Delta = 0.425$ Å for $CuCu_3V_4O_{12}$, meaning that the large Ca^{2+} ions virtually fit the 12-fold oxygen-icosahedral cage, while there is space for the smaller Mn^{2+} and Cu^{2+} ions to move; the presence of the free space is also reflected in the underbonding of A-site cations in $MnCu_3V_4O_{12}$ (BVS = 1.47)[22b] and $CuCu_3V_4O_{12}$ (BVS = 1.09). Especially, $CuCu_3V_4O_{12}$ has the largest A-site cation size mismatch among three compounds, and therefore, it shows the largest value of U_{iso} of A-site cations at 300 K as demonstrated by U_{iso}(Cu1) ≈ 0.045 Å^2 (Table 1), U_{iso} (Mn) ≈ 0.022 Å^2,[22b] and U_{iso}(Ca) ≈ 0.0082 Å^2 (Table S2). The substantial thermal oscillations of small Cu^{2+} ions inside the icosahedral cages allow us to detect the rattling through the C_p measurement. Further studies should be performed to clarify the relation between rattling and physical properties (e.g., electrical conductivity, thermal conductivity, and magnetism).

In conclusion, we have successfully synthesized a novel A-site-ordered quadruple perovskite, $CuCu_3V_4O_{12}$. The low-temperature C_p data, together with the SXRD analysis, show that loosely bound A-site Cu^{2+} ions rattle within the oversized icosahedral cages, with a characteristic temperature of $\Theta_E \approx 55$ K. This is the first observation of rattling in perovskite compounds and also demonstrates a rare example in which 3d transition metals serve as the rattler.

Acknowledgements

The synchrotron radiation experiments were performed at the SPring-8 with the approval of the Japan Synchrotron Radiation Research Institute (Proposal Nos. 2013A1042, 2013A1188, 2013A1689, 2013A1691, and 2014B1135). This research was partly supported by JSPS KAKENHI Grant-in-Aid for Scientific Research (A) (Grant Nos. 25249090 and 25248016) and Scientific Research on Innovative Areas "Nano Informatics" (Grant No. 26106514).

Keywords: cage compounds · high-pressure chemistry · perovskites · rattling · transition metals

How to cite: *Angew. Chem. Int. Ed.* **2015**, *54*, 10870–10874
Angew. Chem. **2015**, *127*, 11020–11024

[1] a) D. Caplin, G. Grüner, J. B. Dunlop, *Phys. Rev. Lett.* **1973**, *30*, 1138; b) D. J. Braun, W. Jeitschko, *J. Less-Common Met.* **1980**, *72*, 147; c) B. Eisenmann, H. Schafer, R. Zagler, *J. Less-Common Met.* **1986**, *118*, 43; d) J. Yamaura, S. Yonezawa, Y. Muraoka, Z. Hiroi, *J. Solid State Chem.* **2006**, *179*, 336.

[2] V. Keppens, D. Mandrus, B. C. Sales, B. C. Chakoumakos, P. Dai, R. Coldea, M. B. Maple, D. A. Gajewski, E. J. Freeman, S. Bennington, *Nature* **1998**, *395*, 876.

[3] Y. Nakai, K. Ishida, H. Sugawara, D. Kikuchi, H. Sato, *Phys. Rev. B* **2008**, *77*, 041101(R).

[4] T. Yanagisawa, P.-C. Ho, M. Yuhasz, M. B. Maple, Y. Yasumoto, H. Watanabe, Y. Nemoto, T. Goto, *J. Phys. Soc. Jpn.* **2008**, *77*, 074607.

[5] B. C. Sales, B. C. Chakoumakos, R. Jin, J. R. Thompson, D. Mandrus, *Phys. Rev. B* **2001**, *63*, 245113.

[6] S. Paschen, W. Carrillo-Cabrera, A. Bentien, V. H. Tran, M. Baenitz, Y. Grin, F. Steglich, *Phys. Rev. B* **2001**, *64*, 214404.

[7] L. Qiu, I. Swainson, G. S. Nolas, M. A. White, *Phys. Rev. B* **2004**, *70*, 035208.

[8] D. Huo, T. Sakata, T. Sasakawa, M. A. Avila, M. Tsubota, F. Iga, H. Fukuoka, S. Yamanaka, S. Aoyagi, T. Takabatake, *Phys. Rev. B* **2005**, *71*, 075113.

[9] K. Umeo, M. A. Avila, T. Sakata, K. Suekuni, T. Takabatake, *J. Phys. Soc. Jpn.* **2005**, *74*, 2145.

[10] K. Suekuni, Y. Takasu, T. Hasegawa, N. Ogita, M. Udagawa, M. A. Avila, T. Takabatake, *Phys. Rev. B* **2010**, *81*, 205207.

[11] Z. Hiroi, S. Yonezawa, T. Muramatsu, J. Yamaura, Y. Muraoka, *J. Phys. Soc. Jpn.* **2005**, *74*, 1255.

[12] M. Brühwiler, S. M. Kazakov, J. Karpinski, B. Batlogg, *Phys. Rev. B* **2006**, *73*, 094518.

[13] T. Dahm, K. Ueda, *Phys. Rev. Lett.* **2007**, *99*, 187003.

[14] K. Matsuhira, C. Sekine, M. Wakeshima, Y. Hinatsu, T. Namiki, K. Takeda, I. Shirotani, H. Sugawara, D. Kikuchi, H. Sato, *J. Phys. Soc. Jpn.* **2009**, *78*, 124601.

[15] J. Yamaura, Z. Hiroi, *J. Phys. Soc. Jpn.* **2011**, *80*, 054601.

[16] D. J. Safarik, T. Klimczuk, A. Llobet, D. D. Byler, J. C. Lashley, J. R. O'Brien, N. R. Dilley, *Phys. Rev. B* **2012**, *85*, 014103.

[17] a) B. C. Sales, M. Mandrus, R. K. Williams, *Science* **1996**, *272*, 1325; b) G. S. Nolas, G. A. Slack, D. T. Morelli, T. M. Tritt, A. C. Ehrlich, *J. Appl. Phys.* **1996**, *79*, 4002; c) J. S. Tse, V. P. Shpakov, V. V. Murashov, V. R. Belosludov, *J. Chem. Phys.* **1997**, *107*, 9271; d) B. C. Sales, D. Mandrus, B. C. Chakoumakos, V. Keppens, J. R. Thompson, *Phys. Rev. B* **1997**, *56*, 15081; e) B. C. Sales, B. C. Chakoumakos, D. Mandrus, *Phys. Rev. B* **2000**, *61*, 2475; f) M. A. Avila, K. Suekuni, K. Umeo, H. Fukuoka, S. Yamanaka, T. Takabatake, *Appl. Phys. Lett.* **2008**, *92*, 041901.

[18] a) F. M. Grosche, H. Q. Yuan, W. Carrillo-Cabrera, S. Paschen, C. Langhammer, F. Kromer, G. Sparn, M. Baenitz, Y. Grin, F. Steglich, *Phys. Rev. Lett.* **2001**, *87*, 247003; b) Y. Nagao, J. Yamaura, H. Ogusu, Y. Okamoto, Z. Hiroi, *J. Phys. Soc. Jpn.* **2009**, *78*, 064702; c) E. D. Bauer, N. A. Frederick, P.-C. Ho, V. S. Zapf, M. B. Maple, *Phys. Rev. B* **2002**, *65*, 100506(R).

[19] a) S. Sanada, Y. Aoki, H. Aoki, A. Tsuchiya, D. Kikuchi, H. Sugawara, H. Sato, *J. Phys. Soc. Jpn.* **2005**, *74*, 246; b) P.-C. Ho, W. M. Yuhasz, N. P. Butch, N. A. Frederic, T. A. Sayles, J. R. Jeffries, M. B. Maple, J. B. Betts, A. H. Lacerda, P. Rogl, G. Giester, *Phys. Rev. B* **2005**, *72*, 094410.

[20] a) B. Bochu, J. Chenavas, J. C. Joubert, M. Marezio, *J. Solid State Chem.* **1974**, *11*, 83; b) M. Lebeau, B. Bochu, J. C. Joubert, J. Chenavas, *J. Solid State Chem.* **1980**, *33*, 257; c) M. A. Subramanian, A. W. Sleight, *Solid State Sci.* **2002**, *4*, 347; d) A. N. Vasil′ev, O. S. Volkova, *Low Temp. Phys.* **2007**, *33*, 895.

[21] a) J. Sánchez-Benítez, J. A. Alonso, M. J. Martínez-Lope, A. De Andrés, M. T. Fernández-Díaz, *Inorg. Chem.* **2010**, *49*, 5679; b) I. Yamada, H. Etani, K. Tsuchida, S. Marukawa, N. Hayashi, T. Kawakami, M. Mizumaki, K. Ohgushi, Y. Kusano, J. Kim, N. Tsuji, R. Takahashi, N. Nishiyama, T. Inoue, T. Irifune, M. Takano, *Inorg. Chem.* **2013**, *52*, 13751.

[22] a) S. V. Ovsyannikov, A. M. Abakumov, A. A. Tsirlin, W. Schnelle, R. Egoavil, J. Verbeeck, G. Van Tendeloo, K. V. Glazyrin, M. Hanfland, L. Dubrovinsky, *Angew. Chem. Int. Ed.* **2013**, *52*, 1494; *Angew. Chem.* **2013**, *125*, 1534; b) Y. Akizuki, I. Yamada, K. Fujita, N. Nishiyama, T. Irifune, T. Yajima, H. Kageyama, K. Tanaka, *Inorg. Chem.* **2013**, *52*, 11538.

[23] B. L. Chamberland, *J. Solid State Chem.* **1970**, *2-2*, 138.

[24] I. D. Brown, D. Altermatt, *Acta Crystallogr. Sect. B* **1985**, *41*, 244.

[25] H. Shiraki, T. Saito, M. Azuma, Y. Shimakawa, *J. Phys. Soc. Jpn.* **2008**, *77*, 064705.

[26] L. S. Kau, D. J. Spira-Solomon, J. E. Penner-Hahn, K. O. Hodgson, E. I. Solomon, *J. Am. Chem. Soc.* **1987**, *109*, 6433.

[27] C. McGuinness, J. E. Downes, P. Sheridan, P. A. Glans, K. E. Smith, W. Si, P. D. Johnson, *Phys. Rev. B* **2005**, *71*, 195111.

[28] S. Zhang, T. Saito, W. T. Chen, M. Mizumaki, Y. Shimakawa, *Inorg. Chem.* **2013**, *52*, 10610.

[29] T. Mizokawa, A. Fujimori, H. Namatame, Y. Takeda, M. Takano, *Phys. Rev. B* **1998**, *57*, 16.

[30] A. Krimmel, A. Günther, W. Kraetscmer, H. Dekinger, N. Büttgen, A. Loidl, *Phys. Rev. B* **2008**, *78*, 165126.

[31] W. Kobayashi, I. Terasaki, J. Takeya, I. Tsukada, Y. Ando, *J. Phys. Soc. Jpn.* **2004**, *73*, 2373.

[32] R. D. Shannon, *Acta Crystallogr. Sect. A* **1976**, *32*, 751.

Received: June 1, 2015
Published online: July 23, 2015

